Long noncoding RNA *SYISL* regulates myogenesis by interacting with polycomb repressive complex 2

Jian Jun Jin[a,b,c,1], Wei Lv[a,b,c,1], Pan Xia[a,b,c], Zai Yan Xu[a,b,c], An Dai Zheng[a,b,c], Xiao Jing Wang[a,b,c], Shan Shan Wang[a,b,c], Rui Zeng[a,b,c], Hong Mei Luo[a,b,c], Guo Liang Li[d,e,f], and Bo Zuo[a,b,c,g,2]

[a]Key Laboratory of Swine Genetics and Breeding of the Ministry of Agriculture and Rural Affairs, Huazhong Agricultural University, 430070 Wuhan, Hubei, People's Republic of China; [b]Key Laboratory of Agriculture Animal Genetics, Breeding and Reproduction of the Ministry of Education, Huazhong Agricultural University, 430070 Wuhan, Hubei, People's Republic of China; [c]Department of Animal Breeding and Genetics, College of Animal Science and Technology, Huazhong Agricultural University, 430070 Wuhan, Hubei, People's Republic of China China; [d]National Key Laboratory of Crop Genetic Improvement, Huazhong Agricultural University, 430070 Wuhan, Hubei, People's Republic of China; [e]Agricultural Bioinformatics Key Laboratory of Hubei Province, Huazhong Agricultural University, 430070 Wuhan, Hubei, People's Republic of China; [f]Department of Big Data Science, College of Informatics, Huazhong Agricultural University, 430070 Wuhan, Hubei, People's Republic of China; and [g]The Cooperative Innovation Center for Sustainable Pig Production, 430070 Wuhan, People's Republic of China

Edited by Se-Jin Lee, University of Connecticut School of Medicine, Farmington, CT, and approved September 11, 2018 (received for review January 26, 2018)

Although many long noncoding RNAs (lncRNAs) have been identified in muscle, their physiological function and regulatory mechanisms remain largely unexplored. In this study, we systematically characterized the expression profiles of lncRNAs during C2C12 myoblast differentiation and identified an intronic lncRNA, *SYISL* (*SYNPO2* intron sense-overlapping lncRNA), that is highly expressed in muscle. Functionally, *SYISL* promotes myoblast proliferation and fusion but inhibits myogenic differentiation. *SYISL* knockout in mice results in significantly increased muscle fiber density and muscle mass. Mechanistically, *SYISL* recruits the enhancer of zeste homolog 2 (EZH2) protein, the core component of polycomb repressive complex 2 (PRC2), to the promoters of the cell-cycle inhibitor gene *p21* and muscle-specific genes such as myogenin (*MyoG*), muscle creatine kinase (*MCK*), and myosin heavy chain 4 (*Myh4*), leading to H3K27 trimethylation and epigenetic silencing of target genes. Taken together, our results reveal that *SYISL* is a repressor of muscle development and plays a vital role in PRC2-mediated myogenesis.

lncRNA | SYISL | PRC2 | H3K27 trimethylation | myogenesis

Myogenesis is a highly ordered process during which muscle stem cell proliferation, migration, differentiation, and fusion are activated to form myofibers (1). This process is controlled by a series of muscle-specific transcription factors, including myogenic differentiation 1 (MyoD), myogenin (MyoG), myogenic factor 5 (Myf5), muscle-specific regulatory factor 4 (MRF4, also known as "Myf6"), and myocyte enhancer factor 2 (MEF2) (2–4). In addition, epigenetic regulators, such as polycomb repressive complex 2 (PRC2), YIN-YANG-1 (YY1), histone deacetylase complexes (HDACs), histone methyltransferase complexes (HMTs), DNA methyltransferase complexes (DNMTs), the SWItch/Sucrose Non-Fermentable complex (SWI/SNF), and lysine methyltransferase 2A (KMT2A), also play crucial roles in muscle development (2, 5–7). Previous studies have shown that myogenic differentiation is associated with global chromatin landscape changes, especially for the well-known repressive marker histone H3 lysine 27 trimethylation (H3K27me3), which participates in the regulation of myogenic differentiation by silencing muscle-specific genes and cell-cycle genes (8, 9). Enhancer of zeste homolog 2 (EZH2), the core component of PRC2, is capable of H3K27me3 and is specifically required for early mouse muscle development (8, 10). Increased EZH2 expression inhibits skeletal muscle cell differentiation by silencing muscle-specific genes (10, 11), and EZH2 is associated with self-renewal of muscle satellite cells and muscle regeneration (12, 13).

Genome-wide analysis of human and mouse genomes has revealed that noncoding RNAs (ncRNAs), including miRNAs, long noncoding RNAs (lncRNAs), Piwi-interacting RNAs, and circular RNAs, are transcribed from most genomes. lncRNAs are defined as RNA molecules greater than 200 nt in length that have negligible protein-coding capacity; they play important roles in the epigenetic regulation of numerous biological processes, including X-chromosome inactivation (14), genome imprinting (15, 16), alternative splicing (17), stem cell maintenance and differentiation (18, 19), and human disease (20–22). During myogenesis, functional lncRNAs, such as *SRA*, *Gtl2/Meg3*, *H19*, *linc-MD1*, *SINE*-containing lncRNAs, *Yam1*, *lncRNA-YY1*, *LncMyoD*, *MALAT1*, *Dum*, *MUNC*, *Linc-RAM*, and *Lnc-mg*, have been found to regulate muscle development and regeneration through diverse mechanisms (23–29). For example, the skeletal muscle-specific overexpression of *lnc-mg* promotes muscle hypertrophy and increases muscle mass (29), and mutation in *H19* leads to significant muscle mass increase in mice (30). Compared with WT mice, *Linc-RAM* and MALAT1-KO mice display impaired and enhanced muscle regeneration, respectively (28, 31). While numerous lncRNAs have been identified in muscle using microarray, high-throughput sequencing, and single-nucleus RNA sequencing (snRNA-seq) analysis (32, 33), most of their roles in myogenesis remain unclear, and many more lncRNAs have yet to be identified.

To systematically identify the lncRNAs that are potentially involved in myogenesis, we characterized the expression profiles of lncRNAs during C2C12 myoblast differentiation using microarray analysis and identified 1,913 differentially expressed lncRNAs. Based on these results, the lncRNA *AK004418*, located in the fourth intron of the *SYNPO2* gene, was identified and named

Significance

While numerous long noncoding RNAs (lncRNAs) have been identified in muscle, most of their roles in myogenesis remain unclear, and many more lncRNAs have yet to be identified. In this study, we identified an intronic lncRNA, *SYISL* (*SYNPO2* intron sense-overlapping lncRNA), which is highly expressed in muscle and interacts directly with polycomb repressive complex 2 (PRC2) to repress muscle development. The results reveal that *SYISL* acts as a regulatory RNA in PRC2-mediated myogenesis.

Author contributions: B.Z. designed research; J.J.J., W.L., P.X., A.D.Z., X.J.W., S.S.W., R.Z., H.M.L., and B.Z. performed research; B.Z. contributed new reagents/analytic tools; J.J.J., W.L., Z.Y.X., G.L.L., and B.Z. analyzed data; and J.J.J., W.L., and B.Z. wrote the paper.

The authors declare no conflict of interest.

This article is a PNAS Direct Submission.

[1]J.J.J. and W.L. contributed equally to this work.

[2]To whom correspondence should be addressed. Email: zuobo@mail.hzau.edu.cn.

This article contains supporting information online at www.pnas.org/lookup/suppl/doi:10.1073/pnas.1801471115/-/DCSupplemental.

Published online October 2, 2018.

"*SYISL*" (for "*SYNPO2* intron sense-overlapping lncRNA"). The *SYISL* gene is highly expressed in skeletal muscle, and its expression increases with C2C12 cell differentiation. Gain- and loss-of-function analysis revealed that *SYISL* promotes myoblast proliferation and inhibits myogenic differentiation. Significantly, *SYISL*-KO mice have more muscle mass and greater muscle fiber density than WT mice. Mechanistically, *SYISL* acts as a regulatory RNA that interacts directly with PRC2 to repress the expression of target genes.

Results

lncRNA and mRNA Expression Profiles During C2C12 Myoblast Differentiation. To systematically identify lncRNAs involved in muscle cell differentiation, we used mRNA and lncRNA microarrays to identify differentially expressed lncRNAs during C2C12 cell differentiation (proliferating myoblasts and myoblasts at 2, 5, and 8 d after cell differentiation, represented as "D0," "D2," "D5," and "D8," respectively). This microarray contained 13,868 lncRNA probes and 19,465 mRNA probes; an overview of the lncRNA and mRNA expression profiles is summarized in Dataset S1. In total, 5,684 lncRNAs and 9,069 mRNA probes with signals in at least 6 of 12 samples had flags in the present or marginal categories (*SI Appendix*, Fig. S1 *A* and *B* and Dataset S1). Among 5,684 lncRNA probes with signals, 4,205 (73.98%) were annotated; intron sense-overlapping lncRNAs accounted for the largest proportion, followed by intergenic and exon sense-overlapping lncRNAs (*SI Appendix*, Fig. S1*C*). The chromosomal distribution of lncRNAs was not uniform; most of the lncRNAs with signals were transcribed from chromosomes 2 and 11 (*SI Appendix*, Fig. S1*D*). Previous studies showed that the expression levels of lncRNAs are highly correlated with those of their adjacent protein-coding genes (34, 35). In this study, we analyzed the expression correlation coefficient (r) of 896 annotated lncRNAs, including natural antisense, intron sense-overlapping, intronic antisense, exon sense-overlapping, and bidirectional lncRNAs, with their adjacent genes and found that 32 lncRNAs showed high expression correlation with their adjacent genes ($|r| > 0.9$; $P < 0.05$) (Dataset S2). Moreover, the expression levels of 12 intergenic lncRNAs were highly correlated with those of their flanking genes ($|r| > 0.6$; $P < 0.05$) (*SI Appendix*, Table S1), suggesting that they possibly exert their functions in *cis*. Next, the expression correlations of four randomly selected lncRNAs (*NR_002864*, *NR_003647*, *AK046046*, and *AK012160*) and their adjacent genes from the microarray data were confirmed by real-time quantitative PCR (qPCR), and the results showed that the r values from both methods were consistent (*SI Appendix*, Fig. S1 *E–I*).

In total, 1,931 lncRNAs and 4,526 mRNAs were identified as being differentially expressed during cell differentiation (fold-change ≥2; $P < 0.05$) (*SI Appendix*, Fig. S1 *J* and *K* and Datasets S3 and S4). Among the differentially expressed lncRNAs, 356 showed gradually increasing expression trends with myoblast differentiation, and 266 were persistently down-regulated during cell differentiation (Fig. 1*A* and Dataset S5). Among the gradually up-regulated lncRNAs, 96 lncRNAs, of which 58 were annotated, were up-regulated more than fivefold between D0 and D8 (Dataset S6). An expression heatmap of the 58 annotated lncRNAs showed that the intron sense-overlapping lncRNA *AK004418* exhibited significantly higher expression than the others and was significantly up-regulated during myogenic differentiation (*SI Appendix*, Fig. S1*L*). *AK004418* is transcribed from the fourth intron of the *SYNPO2* gene (*SI Appendix*, Fig. S2*A*). Consistent with the microarray data, the *SYISL* expression level was increased with C2C12 cell differentiation, as determined by qPCR (Fig. 1*B* and *SI Appendix*, Fig. S2 *B* and *C*). Interestingly, the expression profiles of the *SYISL* gene in multiple adult tissues showed that *SYISL* was highly expressed in muscle tissues such as longissimus dorsi, leg muscle, and tongue

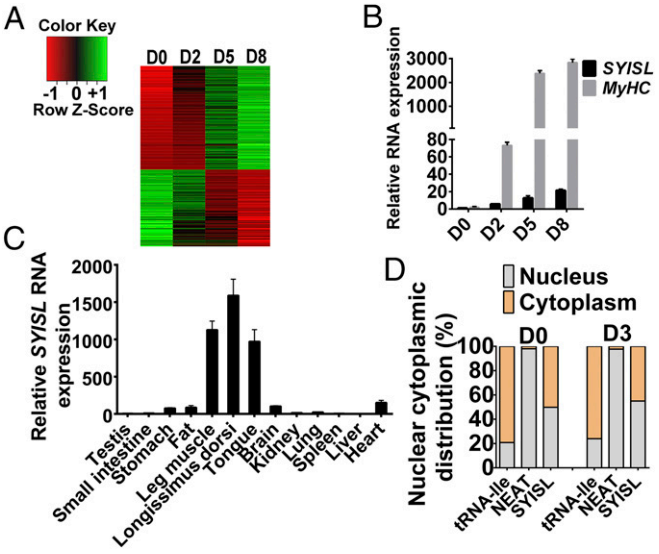

Fig. 1. Characterization of the lncRNA *SYISL* gene. (*A*) Heatmap showing the expression profiles of 356 up-regulated and 266 down-regulated lncRNAs during myogenic differentiation. (*B*) qPCR results showing that *SYISL* and *MyHC* were significantly up-regulated during myogenic differentiation. *MyHC* is the myogenic differentiation marker gene. (*C*) qPCR results showing that *SYISL* was highly expressed in muscle tissues including the longissimus dorsi, leg muscle, and tongue. (*D*) The distribution of *SYISL* in the cytoplasm and nuclei of proliferating C2C12 cells (D0) and C2C12 cells differentiated for 3 d (D3) was determined by qPCR. *NEAT* is a known nuclear lncRNA, and tRNA-Ile is a cytoplasmic-enriched RNA. The relative RNA levels were normalized to those of the control *β-actin*. The data represent the means ± SD of three independent experiments.

when *β-actin*, *GAPDH*, and *18s RNA* were used as reference genes, respectively (Fig. 1*C* and *SI Appendix*, Fig. S2 *D* and *E*). Gene Ontology (GO) analysis showed that *SYISL*-associated genes are clustered mainly into biological adhesion, biological regulation, developmental, metabolic, growth, and immune system processes (*SI Appendix*, Fig. S2 *F* and *G*).

Characterization of the lncRNA *SYISL* and Identification of Its Downstream Target Genes. We first evaluated full-length *SYISL* cDNA in C2C12 cells using RACE and Northern blot assays, confirming that *SYISL* is a 1,181-nt polyadenylated lncRNA deposited in the National Center for Biotechnology Information database (*SI Appendix*, Fig. S2 *H–J*). The coding potential calculator (CPC) software indicated that *SYISL* is a noncoding RNA similar to the known lncRNAs *HOTAIR*, *Braveheart*, and *LncMyoD* (*SI Appendix*, Fig. S2*K*). Cell-fractionation assays demonstrated that *SYISL* is present in both the nuclei and cytoplasm of proliferating and differentiated C2C12 myoblasts (Fig. 1*D*). Furthermore, we examined the expression profiles of *SYISL* during postnatal muscle development, finding up-regulated *SYISL* expression in the first two postnatal weeks and down-regulated *SYISL* expression thereafter (*SI Appendix*, Fig. S2*L*). Because *SYISL* is localized to the fourth intron of the *SYNPO2* gene, we tested the correlation between the spatiotemporal expression patterns of *SYISL* and *SYNPO2* by qPCR. *SYNPO2* was increased during C2C12 cell differentiation before decreasing after 8 d (*SI Appendix*, Fig. S2*M*), and it was mainly expressed in the stomach, small intestine, and heart (*SI Appendix*, Fig. S2*N*), indicating that the spatiotemporal expression patterns of *SYISL* and *SYNPO2* were not consistent. To explore the regulatory mechanisms by which *SYISL* is regulated at the transcriptional level, we conducted luciferase assays with four reporter constructs containing different fragments of *SYISL* promoter (the region between −2000 bp and +200 bp) (*SI Appendix*, Fig. S3*A*).

CELL BIOLOGY

Deletion of the region between −200 bp and +200 bp led to a significant decrease in luciferase activity (*SI Appendix*, Fig. S3*A*). One potential MyoD-binding site (E-box) exists in this region (*SI Appendix*, Fig. S3*B*), and overexpression of *MyoD* increased the luciferase activity of reporter construct D1 containing this E-box (*SI Appendix*, Fig. S3*C*). Meanwhile, knockdown and overexpression of *MyoD* significantly reduced and increased the endogenous *SYISL* expression level, respectively (*SI Appendix*, Fig. S3 *D* and *E*). ChIP results in proliferating and differentiated C2C12 cells showed that MyoD could bind specifically to the E-box between −200 bp and +200 bp (*SI Appendix*, Fig. S3*F*). Therefore, we concluded that *SYISL* is a direct target of the *MyoD* gene.

To screen the target genes regulated by *SYISL*, we designed three RNAi oligonucleotides to knock down the *SYISL* gene specifically; the siRNA-2 fragments had the highest interference efficiency (*SI Appendix*, Fig. S4*A*). We further transfected siRNA-2 to knock down the *SYISL* gene and induced cell differentiation for 2 d. *SYISL* gene expression was significantly reduced when *β-actin*, *GAPDH*, and *18s RNA* were used as reference genes, as indicated by qPCR (*SI Appendix*, Fig. S4*B*). We next used microarrays to analyze genome-wide gene-expression changes after *SYISL* knockdown in C2C12 cells differentiated for 2 d. In total, 399 genes, including *MyoG*, *Myh1*, *Myh2*, *Myh4*, *Myh7*, *Tnni1*, and *Mybpc2*, were significantly up-regulated, and 635 genes were down-regulated after *SYISL* knockdown (fold change >2.0; $P < 0.05$) (*SI Appendix*, Fig. S4*C* and Dataset S7). According to GO enrichment analysis, the differentially expressed genes were mainly related to cellular processes, metabolic processes, biological regulation, and responses to stimuli (*SI Appendix*, Fig. S4 *D* and *E*). Pathway analysis indicated that the up-regulated genes were mainly enriched for muscle differentiation and disease-associated pathways, such as the calcineurin-signaling and chemokine-signaling pathways, dilated cardiomyopathy, and viral myocarditis (*SI Appendix*, Fig. S4*F*). The down-regulated genes, including *CDKs*, *N-Ras*, *ZEB2*, *IGF2BP3*, *Ki67*, and *PCNA*, were mainly involved in axon guidance, the cell cycle, and MAPK-signaling pathways (*SI Appendix*, Fig. S4*G*). To validate the microarray results, we used qPCR to confirm the expression changes of some differentially expressed genes after *SYISL* overexpression and knockdown in C2C12 cells; the results from both techniques were consistent (*SI Appendix*, Fig. S4 *H–K*). From the above results, we deduced that *SYISL* might be involved in the regulation of myoblast proliferation and differentiation.

***SYISL* Promotes Myoblast Proliferation and Fusion but Inhibits Myogenic Differentiation.** To determine whether the *SYISL* gene is involved in myogenesis, we used functional gain and loss to study the effects of *SYISL* on myoblast proliferation and differentiation in C2C12 cells. First, we used RTCA xCELLigence, 5-ethynyl-2′-deoxyuridine (EdU) staining, and flow cytometry assays to verify the potential roles of *SYISL* in C2C12 cell proliferation. The RTCA xCELLigence assay showed that *SYISL* knockdown significantly reduced the cell-proliferation capacity after 30 h of transfection, whereas *SYISL* overexpression markedly improved the cell-proliferation capacity after 40 h of transfection (Fig. 2*A* and *SI Appendix*, Fig. S5*A*). The EdU staining assay showed that *SYISL* knockdown significantly decreased EdU incorporation, and *SYISL* overexpression resulted in increased EdU positivity compared with that of the control (Fig. 2*B* and *SI Appendix*, Fig. S5*B*). Flow cytometry analysis indicated a significant reduction in the percentage of S-phase cells after *SYISL* knockdown, and opposite effects were observed after the overexpression of *SYISL* (Fig. 2*C* and *SI Appendix*, Fig. S5*C*). These results suggested that *SYISL* accelerates myoblast proliferation. In addition, we detected the expression of the key proliferation marker gene *Ki67* after overexpression and knockdown of *SYISL*. The Ki67 protein was significantly down-regulated after *SYISL* knockdown, and *SYISL* overexpression promoted its protein expression, while no significant difference at the protein level was observed for *SYNPO2* gene expression (Fig. 2*D* and *SI Appendix*, Fig. S5*D*).

Next, we investigated the role of *SYISL* in myogenic differentiation. Real-time PCR, Western blot, and immunofluorescence staining were performed to detect the expression of myogenic marker genes including *MyoD*, *MyoG*, and *MyHC*. *SYISL* was successfully knocked down in C2C12 cells at D0, D2, D4, and D6 (*SI Appendix*, Fig. S6*A*). *SYISL* knockdown significantly promoted the myogenic differentiation of C2C12 cells, as demonstrated by the increased mRNA and protein expression of the myogenic marker genes *MyoG* and *MyHC* (Fig. 2 *E–G* and *SI Appendix*, Fig. S6 *B* and *C*). However, no significant change in protein expression of the *MyoD* gene was found after *SYISL* knockdown (Fig. 2*E*). Likewise, *SYNPO2* expression was detected after *SYISL* knockdown; no significant differences were observed at either the mRNA or protein level (Fig. 2*E* and *SI Appendix*, Fig. S6*D*). To further confirm the knockdown results, we overexpressed the *SYISL* gene in C2C12 cells and then induced their differentiation. As expected, *SYISL* overexpression significantly decreased the expression of *MyoG* and *MyHC* at the mRNA and protein levels, but no significant changes in the expression of the *MyoD* and *SYNPO2* genes were observed after *SYISL* overexpression (*SI Appendix*, Figs. S6 *E–H* and S7 *A–C*).

Finally, myosin immunofluorescence staining was used to analyze the function of *SYISL* in the regulation of myotube fusion. *SYISL* knockdown increased the proportion of myotubes with three or fewer nuclei (Fig. 2*H*) and decreased the mRNA expression of the fusion marker genes *Myomaker* and *β-1integrin* (*SI Appendix*, Fig. S7*D*), while *SYISL* overexpression increased the proportion of myotubes with more than three cell nuclei (*SI Appendix*, Fig. S7*E*) and promoted the mRNA expression levels of *Myomaker* and *β-1 integrin* (*SI Appendix*, Fig. S7*F*), suggesting that *SYISL* facilitates more myoblast fusion into one myotube. Moreover, we used the wound-healing test to determine the cell migration capacity at 12, 24, and 48 h after the knockdown or overexpression of *SYISL* in C2C12 cells. *SYISL* knockdown significantly promoted myoblast migration, and *SYISL* overexpression inhibited cell migration (*SI Appendix*, Fig. S8 *A* and *B*).

***SYISL* KO in Mice Significantly Increases Muscle Fiber Density, Muscle Mass, and Regeneration.** To determine the role of *SYISL* in muscle development at the individual animal level, we used CRISPR/Cas9-mediated genome editing to generate *SYISL*-KO mice. A 1,133-bp genomic region that contains most of the *SYISL* transcript was deleted, and different genotypes were identified by PCR (*SI Appendix*, Fig. S9*A*). *SYISL*-KO mice were healthy and manifested no significant differences in weight or growth rate compared with WT mice (*SI Appendix*, Fig. S9*B*). qPCR results showed that *SYISL* expression was barely detectable in the skeletal muscles of the *SYISL*-KO mice (*SI Appendix*, Fig. S9*C*). To validate the effects of *SYISL* depletion on muscle development, we examined the expression changes of the proliferation and myogenic marker genes in the skeletal muscles of 2-mo-old WT and *SYISL*-KO mice. Compared with WT mice, *SYISL*-KO mice displayed higher protein expression levels of MyoG and MyHC but lower protein expression levels of N-Ras (*SI Appendix*, Fig. S9*D*). Moreover, the protein expression of the *SYNPO2* gene was not significantly altered (*SI Appendix*, Fig. S9*D*), a finding that was consistent with the results in C2C12 cells.

Although the *SYISL*-KO mice showed normal growth and body weight, the weights of their gastrocnemius (Gas), tibialis anterior (TA), and quadriceps (Qu) muscles in both males and females were significantly higher than those of WT mice (Fig. 3*A* and *SI Appendix*, Fig. S9*E*). Next, we used H&E staining and immunohistochemistry staining to assess changes in the number and size of myofibers. Compared with WT mice, *SYISL*-KO mice showed a significantly lower mean cross-sectional area of individual myofibers but a significantly higher number of myofibers/mm^2 and a

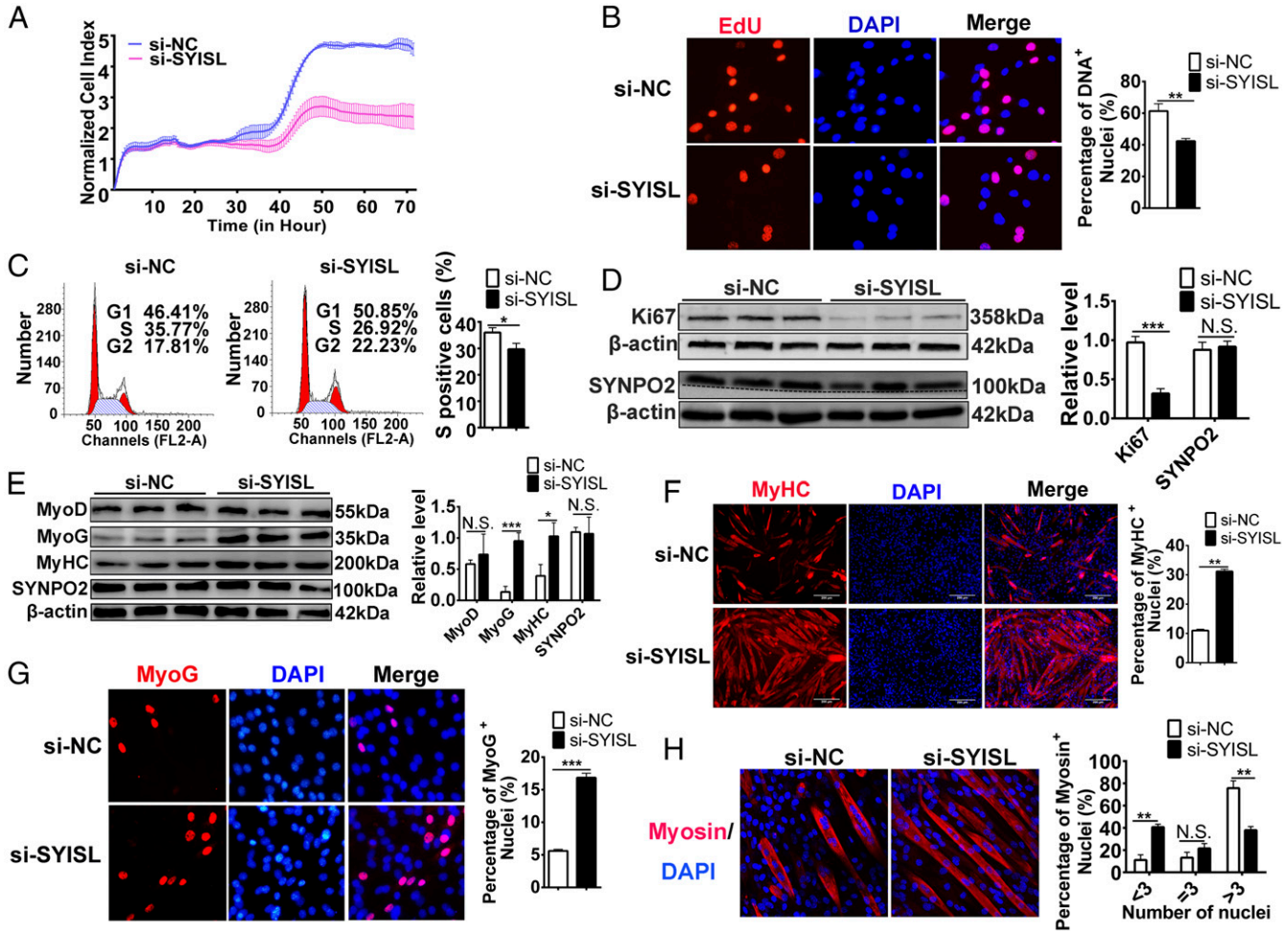

Fig. 2. *SYISL* promotes myoblast proliferation and fusion but inhibits myogenic differentiation. (*A*) RTCA xCELLigence analysis showed that C2C12 cell-proliferation capacity was significantly reduced after *SYISL* knockdown. (*B*) Representative photographs of EdU staining showing that *SYISL* knockdown significantly decreased EdU incorporation. Nuclei were stained with DAPI, magnification 40×. (*C*) Flow cytometry analysis showing that *SYISL* knockdown significantly decreased the percentage of S-phase cells. (*D*) Western blot results showing that *SYISL* knockdown significantly decreased the protein expression level of Ki67, while no significant difference for SYNPO2 protein expression was observed in proliferating C2C12 cells. The dotted line represents a dividing line. Below the dividing line is white space. (*E*) Western blot results showing that *SYISL* knockdown significantly increased the protein expression levels of MyoG and MyHC in C2C12 cells differentiated for 2 d but did not affect MyoD and SYNPO2 protein expression. (*F*) Representative photographs of MyHC immunofluorescence staining in C2C12 cells differentiated for 4 d showing that *SYISL* knockdown promoted myoblast differentiation. Positively stained cells were quantified, magnification 10×. (*G*) Representative photographs of MyoG immunofluorescence staining in C2C12 cells differentiated for 2 d showing that *SYISL* knockdown significantly promoted the MyoG protein expression level. Positively stained cells were quantified, magnification 40×. (*H*) Representative photographs of myosin immunofluorescence staining in C2C12 cells differentiated for 5 d showing that *SYISL* knockdown decreased the fusion rate of myoblasts, magnification 40×. The relative protein levels were normalized to those of the control *β-actin*. The data represent the means ± SD of three independent experiments. $*P < 0.05$, $**P < 0.01$, $***P < 0.001$. NC, negative control; N.S. indicates statistical nonsignificance.

higher proportion of smaller myofibers (Fig. 3*B* and *SI Appendix*, Figs. S9 *F–I* and S10 *A–E*). Next, we scanned the whole cross-section of the TA muscle from *SYISL*-KO and WT mice and found that the TA muscle from *SYISL*-KO mice had a higher total fiber number than that of WT mice (Fig. 3*C*). To further confirm the roles of *SYISL* in cell proliferation, differentiation, and fusion, we isolated muscle primary myoblasts from the leg muscles of WT and *SYISL*-KO mice. The 3-(4,5-dimethylthiazol-2-yl)-2,5-diphenyltetrazolium bromide (MTT) and RTCA xCELLigence assays showed that the proliferation capacity of *SYISL*-KO muscle primary myoblasts was significantly lower than that of WT cells (Fig. 3 *D* and *E*). Similarly, the EdU staining assay showed that *SYISL* KO in myoblasts significantly decreased EdU staining (Fig. 3*F*). Moreover, *SYISL* KO significantly decreased *Ki67* and *N-Ras* gene mRNA expression but did not affect *Pax7* gene expression (*SI Appendix*, Fig. S11*A*). Next, we analyzed the effects of *SYISL* deletion on the differentiation of primary myoblasts; the results showed that deletion of *SYISL* in primary myoblasts significantly promoted *MyoG* and *MyHC* mRNA expression, but the expression of *MyoD* was not significantly altered, a finding that was consistent with the results in C2C12 cells (*SI Appendix*, Fig. S11*B*). MyHC, MyoG, and myosin immunofluorescence staining further showed that *SYISL* KO in primary myoblasts significantly increased myogenic differentiation and the number of myotubes but decreased the myoblast fusion rate as judged by fewer cell nuclei in each myotube (Fig. 3*G* and *SI Appendix*, Fig. S11 *C* and *D*). These data suggested that *SYISL* promotes myoblast proliferation, increases myoblast fusion, and inhibits differentiation in vivo and in vitro.

To investigate the role of *SYISL* in postnatal muscle regeneration, we performed a cardiotoxin (CTX)-induced muscle-injury experiment in WT and *SYISL*-KO mice. H&E staining of muscle sections at different times of injury showed that at 14 and 18 d following CTX injection most of the inflammatory myofibers in *SYISL*-KO mice had been replaced by newly formed ones with

CELL BIOLOGY

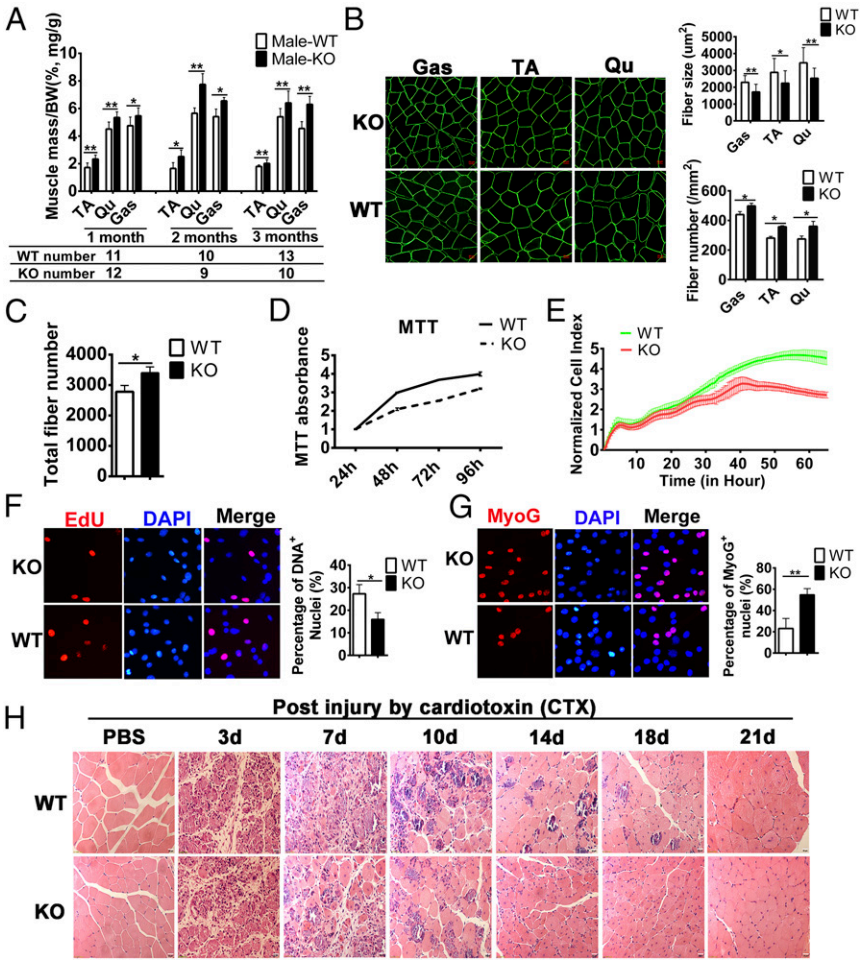

Fig. 3. *SYISL* KO in mice results in increased muscle fiber density, muscle mass, and regeneration. (*A*) The weights of the Gas, TA, and Qu muscles of male *SYISL*-KO mice were significantly higher than those of male WT mice. All the data were normalized to the body weight (mg/g). (*B*) Representative photographs of immunohistochemistry staining of dystrophin for Gas, TA, and Qu muscles from 2-mo-old *SYISL*-KO and WT mice. Compared with WT mice, *SYISL*-KO mice had lower average cross-sectional areas and more muscle fibers/mm^2, magnification 40×. (*C*) *SYISL*-KO mice had more total muscle fibers than WT mice. The TA muscle was isolated from *SYISL*-KO and WT mice, and immunohistochemistry was performed using the anti-dystrophin antibody. The number of muscle fibers was measured by scanning the whole cross-section. (*D*–*F*) *SYISL* KO significantly decreased primary myoblast proliferation capacity as determined by MTT (*D*), RTCA xCELLigence analysis (*E*), and EdU staining (*F*), magnification 40×. (*G*) Representative photographs of MyoG immunofluorescence staining showing that *SYISL* KO in primary myoblasts significantly increased the myogenic differentiation, magnification 40×. (*H*) Representative photographs of H&E staining of GAS muscle at days 3, 7, 10, 14, 18, and 21 after injury showing that *SYISL*-KO mice with smaller myofibers complete muscle damage repair earlier than WT mice with larger myofibers. PBS was used as the control, magnification 40×. The data represent the means ± SD of at least three independent experiments. **P* < 0.05, ***P* < 0.01.

centralized nuclei, but more inflammatory cells and necrotic myofibers still existed in WT mice. At day 21 after CTX injection, muscle regeneration and repair were completed in *SYISL*-KO mice, but newly formed myofibers identified by the presence of central nuclei were still present in WT mice. Moreover, the regenerated myofibers in *SYISL*-KO mice were denser and smaller than those in WT mice, which were similar to the uninjured state (Fig. 3*H*). To confirm these findings, we examined the expression of embryonic MyHC (eMyHC), a marker of muscle regeneration, at day 14 and day 21 after CTX injection. At these two stages, regenerating myofibers of WT mice exhibited higher eMyHC expression than those of *SYISL*-KO mice (*SI Appendix*, Fig. S12*A*). These results indicated that muscle regeneration in WT mice lags behind that of *SYISL*-KO mice. Muscle regeneration involves the activation and proliferation of satellite cells, followed by their terminal differentiation. To investigate how *SYISL* regulates muscle regeneration, we conducted Pax7 (a specific maker of muscle satellite cells), EdU, and MyoG staining to compare proliferation and differentiation capacities of satellite cells in the regenerating myofibers from WT and *SYISL*-KO mice at day 3 after injury. Consistent with the above results in cells, the percentage of proliferating muscle satellite cells (Pax7$^+$/EdU$^+$) decreased by about 27% in *SYISL*-KO mice compared with that in WT mice while no significant change was found in the percentage of satellite (Pax7$^+$) cells (*SI Appendix*, Fig. S12*B*). In addition, the results of Pax7 and dystrophin staining in normal muscle tissues indicated that there was no significant difference in the total number of satellite cells in WT and *SYISL*-KO mice (*SI Appendix*, Fig. S12*C*). These results suggested that *SYISL* KO does not affect the Pax7 level but induces cell-cycle exit and prevents the expansion of satellite cells. Meanwhile, differentiated (MyoG$^+$) cells increased by about 72% in *SYISL*-KO mice compared with WT mice (*SI Appendix*, Fig. S12*D*), suggesting an earlier myogenic differentiation potential of *SYISL*-KO satellite cells. Considering the opposing effects of *SYISL* on satellite cell proliferation and differentiation during muscle regeneration, we infer that the faster muscle-damage repair in *SYISL*-KO mice may be mainly attributable to the more efficient differentiation of *SYISL*-KO satellite cells. Additionally, it is also possible that the smaller myofibers in *SYISL*-KO mice require less time to regenerate than the larger myofibers in WT mice.

***SYISL* Interacts Directly with PRC2.** The nuclear localization of *SYISL* suggested that this lncRNA may recruit RNA-binding proteins to control the transcription of target genes. Thus, we attempted to identify the protein partners of *SYISL*. First, the potential *SYISL*-binding proteins were predicted using the catRAPID algorithm, and EZH2 was found to interact with *SYISL* (*SI Appendix*, Fig. S13*A*), a finding that was also confirmed by RNA–protein interaction prediction (RPISeq) (*SI Appendix*, Fig. S13*B*). Previous studies have shown that EZH2 interacts with various regulatory lncRNAs and plays important roles in myogenesis (25, 36). To confirm the roles of the *EZH2* gene in myoblast proliferation and myogenic differentiation, we examined EZH2 protein expression during C2C12 cell differentiation and found that the EZH2 expression level was decreased with C2C12 cell differentiation (*SI Appendix*, Fig. S13*C*). Next, we overexpressed and knocked down the *EZH2* gene in C2C12 cells. As expected,

overexpression of the *EZH2* gene significantly promoted cell proliferation and decreased myogenic differentiation (*SI Appendix*, Fig. S13 *D–F*), which were confirmed by the results of *EZH2* gene knockdown (*SI Appendix*, Fig. S13*G*). To further elucidate the possible association of *SYISL* with EZH2, we compared the target genes of *SYISL* with EZH2 and H3K27me3 ChIP-seq data from C2C12 myoblasts. In total, 88 target genes regulated by *SYISL* overlapped with H3K27me3 target genes, and 36 genes overlapped with EZH2 target genes (*SI Appendix*, Fig. S13*H* and Dataset S8). Also, *MyoG*, *Myh4*, and *MCK* promoters were enriched by endogenous EZH2 and H3K27me3, as determined by ChIP in proliferating and differentiated C2C12 cells (*SI Appendix*, Fig. S13 *I* and *J*). To validate this interaction between *SYISL* and EZH2, we performed RNA immunoprecipitation (RIP) of EZH2. As expected, EZH2 pulled down *SYISL* in C2C12 cell lysates, suggesting that EZH2 interacts with *SYISL* in vivo (Fig. 4*A*). To further determine this specific interaction in vitro, we performed a biotinylated RNA-pulldown assay using biotinylated *SYISL* with biotinylated single-stranded antisense RNA as the control. Indeed, *SYISL* RNA could bind EZH2, but the antisense RNA strand pulled down no EZH2 protein (Fig. 4*B*). In conclusion, *SYISL* interacts specifically with EZH2 in C2C12 cells in vitro and in vivo.

To determine the core protein-binding domain of *SYISL*, we constructed a series of truncated *SYISL* fragments. Unlike full-length *SYISL*, none of the truncated fragments could physically bind EZH2 (Fig. 4*C*). We next investigated the role of truncated fragments and full-length *SYISL* in myoblast proliferation and differentiation. Only the full-length *SYISL* significantly promoted cell proliferation, as shown by EdU staining (Fig. 4*D*), and significantly increased the expression of *Ki67*, *N-Ras*, and *CDK6* genes (*SI Appendix*, Fig. S13*K*). Similarly, only full-length *SYISL* significantly repressed myogenic differentiation, as shown by MyHC immunofluorescence staining (Fig. 4*E*), and *MyoG* and *MyHC* gene expression (*SI Appendix*, Fig. S13*L*). These results supported the notion that full-length *SYISL* is required to exert its function in its physical interaction with EZH2. PRC2 is a multisubunit histone methyltransferase complex mainly including EZH2, SUZ12, EED, and RBBP4 (37, 38). To verify whether *SYISL* could interact with other members of the PRC complex, such as SUZ12, we performed RNA-pulldown and RIP experiments. The full-length *SYISL* interacted with SUZ12 (Fig. 4 *F* and *G*). This interaction of PRC2 and *SYISL* was also confirmed by their nuclear colocalization as shown by *SYISL* RNA FISH and EZH2/SUZ12 immunofluorescence staining (Fig. 4*H*). These results suggested that *SYISL* specifically recruits PRC2 to perform its epigenetic regulation roles.

SYISL Regulates Myogenesis by Recruiting PRC2 to the Promoters of Target Genes. Because *SYISL* specifically interacts with PRC2, we investigated whether there is a mutual regulation relationship between *SYISL* and EZH2 in C2C12 cells. The results showed that *SYISL* knockdown or overexpression did not significantly influence EZH2 gene expression (*SI Appendix*, Fig. S14 *A–D*), nor was *SYISL* gene expression significantly altered by EZH2 knockdown or overexpression (*SI Appendix*, Fig. S14 *E* and *F*). Similarly, knockdown of *SYISL* did not influence *SUZ12* gene expression (*SI Appendix*, Fig. S14*G*). These results suggested that *SYISL* regulates myogenesis through its interaction with PRC2 rather than by regulating *EZH2* gene expression. Because EZH2 functions by binding to target promoters, we performed

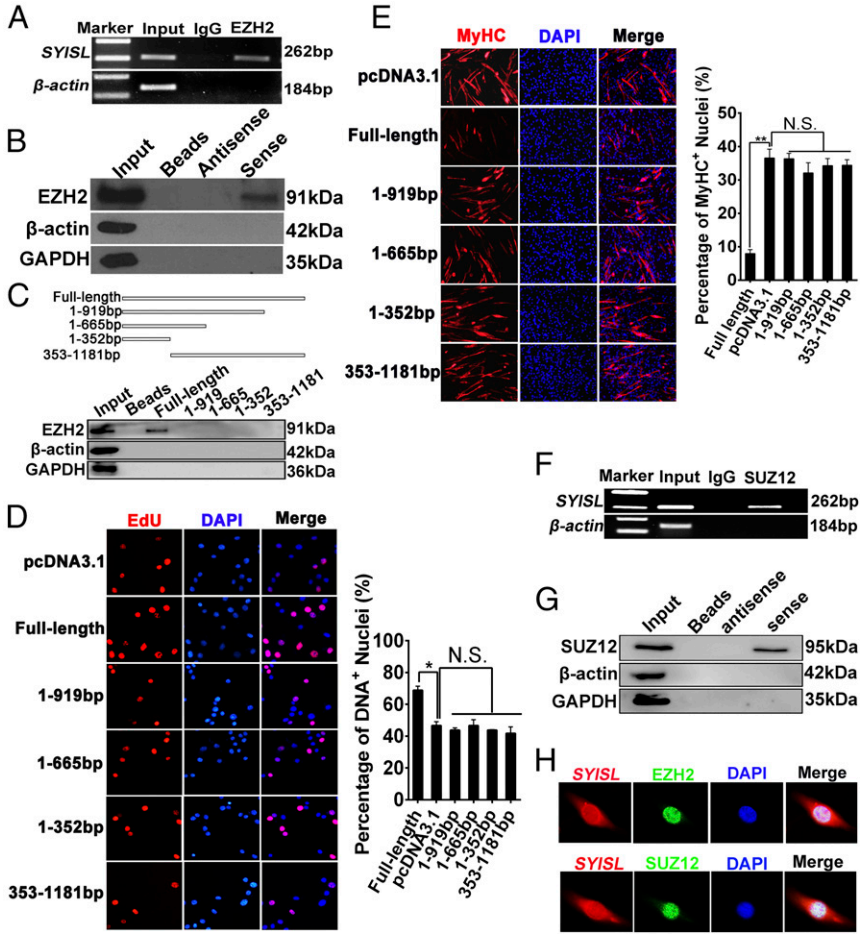

Fig. 4. *SYISL* interacts directly with PRC2. (*A* and *B*) Interaction between *SYISL* and EZH2 as determined by RIP (*A*) and biotin-labeled RNA pulldown (*B*). (*C*) The interaction of full-length and truncated *SYISL* (base pairs 1–352, 1–665, 1–919, and 353–1181) with EZH2 was determined by RNA pulldown. (*D*) Representative photographs of EdU staining in proliferating C2C12 cells and quantification showing that only full-length SYISL significantly promoted myoblast proliferation, magnification 40×. (*E*) Representative photographs of MyHC immunofluorescence staining in C2C12 cells differentiated for 2 d and quantification showing that only full-length SYISL significantly repressed myoblast differentiation, magnification 10×. (*F* and *G*) Interaction between *SYISL* and SUZ12 as determined by RIP (*F*) and biotin-labeled RNA pulldown (*G*). (*H*) RNA FISH and immunofluorescence staining showed that *SYISL* colocalized with EZH2 and SUZ12 in C2C12 cell nuclei, magnification 63×. *GAPDH* and *β-actin* were used as negative controls in RIP and RNA pulldown, respectively. The values are shown as means ± SD of three independent experiments. $*P < 0.05$, $**P < 0.01$. N.S. indicates statistical nonsignificance.

CELL BIOLOGY

ChIP to elucidate whether *SYISL* affects the capacity of EZH2 to bind the promoters of its target myogenic genes such as *MyoG*, *Myh4*, and *MCK* in C2C12 cells. *SYISL* overexpression significantly increased and *SYISL* knockdown significantly decreased the enrichment of EZH2 at *MyoG*, *Myh4*, and *MCK* gene promoters (Fig. 5 *A* and *B*). Previous studies revealed that EZH2 repressed gene expression by binding chromatin and establishing H3K27me3 (10). Thus, we performed ChIP analysis for H3K27me3 after *SYISL* overexpression and knockdown in C2C12 cells, finding that *SYISL* overexpression significantly increased and *SYISL* knockdown significantly decreased H3K27me3 enrichment at the *MyoG*, *Myh4*, and *MCK* promoters (Fig. 5 *C* and *D*). To substantiate these observations, we conducted EZH2 and H3K27me3 ChIP assays in the primary myoblasts from *SYISL*-KO and WT mice and found that there was no significant enrichment of EZH2 and H3K27me3 at *MyoG*, *Myh4*, and *MCK* promoters in *SYISL*-KO primary myoblasts compared with levels in WT primary myoblasts (Fig. 5 *E* and *F*), indicating that *SYISL* KO results in the removal of EZH2 and H3K27me3 from target promoters. Because overexpression of *SYISL* led to the down-regulation of the *MyoG* expression level, we tested whether *MyoG* could efficiently rescue the expression of myogenic genes after overexpression of *SYISL*. Remarkably, *MyoG* overexpression rescued the inhibitory effects of myogenic gene expression mediated by *SYISL* overexpression (Fig. 5*G* and *SI Appendix*, Fig. S14 *H* and *I*). The *SYISL* regulation of myogenic differentiation through *MyoG* function was also confirmed by the bioinformatics analysis of the *SYISL* target genes with MyoG and MyoD ChIP-seq data from C2C12 myoblasts. In total, 422 target genes regulated by *SYISL* overlapped with both MyoG and MyoD target genes, 108 genes regulated by *SYISL* specifically overlapped with MyoG target genes, and only 26 genes that may be regulated by *SYISL* through other mechanisms or in an indirect manner overlapped with MyoD target genes (*SI Appendix*, Fig. S14*J* and Dataset S9). In conclusion, *SYISL* inhibits myogenic differentiation by recruiting PRC2 to the promoters of myogenic genes.

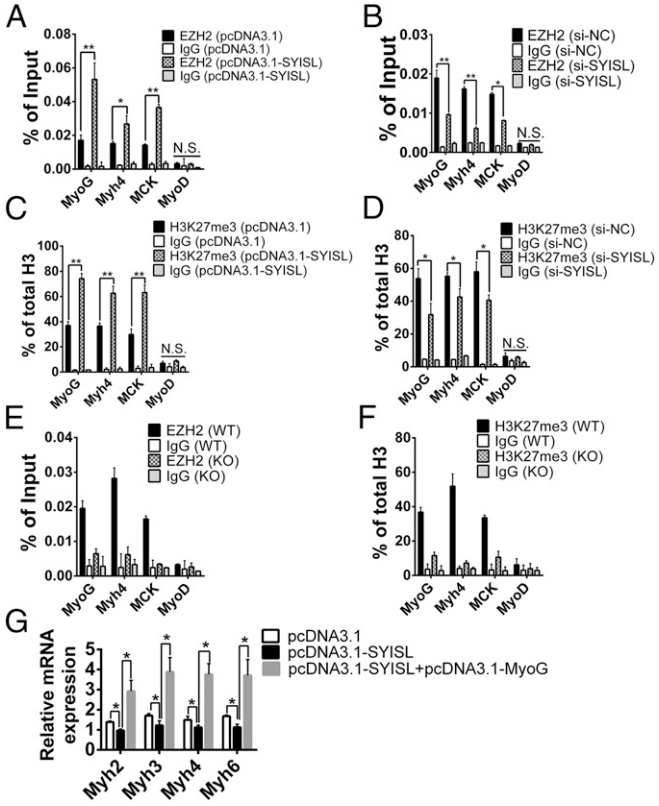

Fig. 5. *SYISL* inhibits myogenic differentiation by recruiting EZH2 and H3K27me3 to the promoters of myogenic genes. (*A*) ChIP-qPCR results showing that *SYISL* overexpression significantly increased EZH2 enrichment at the *MyoG*, *Myh4*, and *MCK* promoters in C2C12 cells differentiated for 3 d. (*B*) ChIP-qPCR results showing that *SYISL* knockdown significantly decreased EZH2 enrichment at the *MyoG*, *Myh4*, and *MCK* promoters in C2C12 cells differentiated for 3 d. (*C*) ChIP-qPCR results showing that *SYISL* overexpression significantly increased H3K27me3 enrichment at the *MyoG*, *Myh4*, and *MCK* promoters in C2C12 cells differentiated for 3 d. (*D*) ChIP-qPCR results showing that *SYISL* knockdown significantly decreased H3K27me3 enrichment at the *MyoG*, *Myh4*, and *MCK* promoters in C2C12 cells differentiated for 3 d. (*E* and *F*) ChIP-qPCR results in primary myoblasts showing that there was no significant enrichment of EZH2 (*E*) or H3K27me3 (*F*) at *MyoG*, *Myh4*, and *MCK* promoters in *SYISL*-KO primary myoblasts differentiated for 3 d compared with levels in WT primary myoblasts. (*G*) qPCR results showing that *MyoG* overexpression rescued the inhibitory effects of myogenic gene expression mediated by *SYISL* overexpression. The relative RNA levels were normalized to those of the control *β-actin*. The values are shown as means ± SD of three independent experiments. $*P < 0.05$, $**P < 0.01$. N.S. indicates statistical nonsignificance.

Recent studies have reported that some lncRNAs, including *Xist*, *APTR*, and *ANCR*, can recruit EZH2 to epigenetically silence the *cdkn1a* (cyclin-dependent kinase inhibitor 1A, *p21*) gene, thereby promoting cell proliferation (39–41). *p21* is an important cell-cycle regulator that restrains the cell cycle by inhibiting *CDK*s in mouse embryonic fibroblasts (42, 43). In this study, the inhibitory effects of *p21* on cell proliferation were confirmed by EdU staining in C2C12 cells (*SI Appendix*, Fig. S14*K*). Thus, we deduced that *SYISL* may recruit EZH2 to inhibit *p21* gene expression, thereby promoting myoblast proliferation. First, we investigated the effects of *SYISL* on the expression of *p21* in C2C12 cells; the results indicated that *SYISL* significantly inhibited *p21* gene expression and increased the expression of *CDK6*, its downstream target gene, at either the mRNA or the protein level (Fig. 6 *A* and *B* and *SI Appendix*, Fig. S14 *L* and *M*). Consistent with these results, deletion of *SYISL* in mice resulted in significantly increased p21 protein expression in muscle (Fig. 6*C*). Additionally, we analyzed the effects of the *EZH2* gene on *p21* gene expression in myoblasts. Similar to *SYISL*, *EZH2* inhibited *p21* gene expression and increased *CDK6* gene expression (*SI Appendix*, Fig. S14*N*). Next, we analyzed the effects of *SYISL* on the capacity of EZH2 and H3K27me3 to bind the *p21* gene promoter in C2C12 cells. As expected, *SYISL* overexpression significantly promoted EZH2 and H3K27me3 enrichment at the *p21* promoter (Fig. 6 *D* and *E*), while *SYISL* knockdown reduced EZH2 and H3K27me3 enrichment at the *p21* promoter (Fig. 6 *F* and *G*). Consistently, no enrichment of EZH2 and H3K27me3 at the *p21* promoter was found in *SYISL*-KO primary myoblasts, while the *p21* promoter was significantly enriched by EZH2 and H3K27me3 in WT primary myoblasts (Fig. 6 *H* and *I*). Taken together, these results indicate that *SYISL* inhibits *p21* gene expression by recruiting EZH2 to the *p21* promoter, ultimately resulting in failure to exit the cell cycle. To further confirm whether *SYISL* promotes the cell cycle through the *p21* pathway, we cotransfected *SYISL* and *p21* into C2C12 cells. The results showed that overexpression of *SYISL* induced the expression of *CDK*, *N-Ras*, and *Ki67* genes. However, *p21* overexpression significantly attenuated *SYISL* activity (Fig. 6*J*). These results demonstrated that the *p21* gene is the main downstream target gene in the regulation of cell proliferation by *SYISL*.

To confirm whether *SYISL* binds directly to the promoters of its target genes, we examined *SYISL* enrichment at the *MyoG*, *p21*, *Myh4*, *MCK*, and *MyoD* promoters by chromatin isolation by RNA purification (ChIRP) in C2C12 cells and primary myoblasts. The promoters of *MyoG*, *p21*, *Myh4*, and *MCK*, but not *MyoD*, were significantly enriched in *SYISL* ChIRP compared with the lacZ RNA controls (Fig. 6 *K* and *L*). These data confirmed that *SYISL* physically binds to the promoters of target genes and inhibits their transcription by recruiting PRC2. Finally, to test whether *SYISL* is required for the EZH2-mediated epigenetic

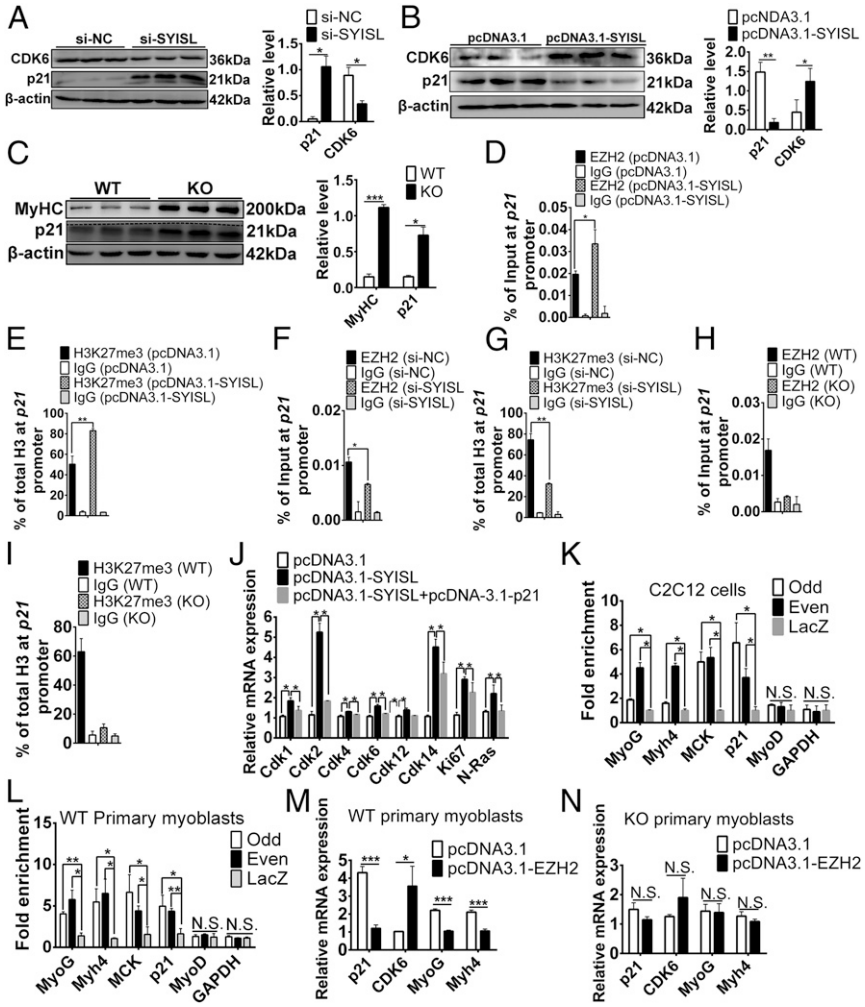

Fig. 6. *SYISL* promotes cell proliferation by epigenetically repressing the *p21* gene. (*A*) Western blot results showing that *SYISL* knockdown significantly increased p21 protein expression and decreased CDK6 protein expression in proliferating C2C12 cells. The *CDK6* gene is a known *p21* target gene. (*B*) Western blot results showing that *SYISL* overexpression inhibited p21 protein expression and increased CDK6 protein expression in proliferating C2C12 cells. (*C*) Western blot results showing that *SYISL* KO in mice significantly increased p21 protein expression in muscle. The dotted line represents a dividing line. Above the dividing line is white space. (*D* and *E*) ChIP-qPCR results showing that *SYISL* overexpression significantly increased EZH2 (*D*) and H3K27me3 (*E*) enrichment at the *p21* promoter in proliferating C2C12 cells. (*F* and *G*) ChIP-qPCR results showing that *SYISL* knockdown significantly decreased EZH2 (*F*) and H3K27me3 (*G*) enrichment at the *p21* promoter in proliferating C2C12 cells. (*H* and *I*) ChIP-qPCR results showing that there was no significant enrichment of EZH2 (*H*) or H3K27me3 (*I*) at the *p21* promoter in *SYISL*-KO primary myoblasts compared with levels in WT primary myoblasts. (*J*) qPCR results showing that *p21* overexpression significantly attenuated *SYISL* activity. (*K* and *L*) ChIRP-qPCR results showing that *SYISL* could physically bind to the *MyoG*, *Myh4*, *MCK*, and *p21* promoters, but not to the *MyoD* promoter, in C2C12 cells (*K*) and primary myoblasts (*L*). Probes against *lacZ* RNA were used as a negative control. Twelve probes tiling the full-length of SYISL RNA were separated into odd and even pools. (*M* and *N*) qPCR results showing that *EZH2* gene overexpression significantly inhibited *p21*, *MyoG*, and *Myh4* gene expression and increased *CDK6* expression in WT primary myoblasts (*M*), but no significant changes were found in *SYISL*-KO primary myoblasts (*N*). The relative RNA and protein levels were normalized to those of the control *β-actin*. The values are shown as the means ± SD of three independent experiments. $*P < 0.05$, $**P < 0.01$, $***P < 0.001$. NC, negative control; N.S. indicates statistical nonsignificance.

silencing of muscle-specific genes and cell-cycle genes, we performed *EZH2* gene overexpression experiments in primary myoblasts from WT and *SYISL*-KO mice. As expected, *EZH2* gene overexpression significantly inhibited *p21*, *MyoG*, and *Myh4* gene expression and increased *CDK6* expression in WT primary myoblasts (Fig. 6*M*), while no significant differences in the expression levels of these genes were detected in *SYISL*-KO primary myoblasts (Fig. 6*N*).

Discussion

Recent studies have highlighted the importance of lncRNAs in diverse biological processes, most specifically in regulating cell proliferation and differentiation (44, 45). The expression levels of lncRNA are found to be more tissue- and cell type-specific than those of protein-coding genes, and lncRNAs have been shown to be differentially expressed across various stages of differentiation, indicating that they may be fine-tuners of cell fate (44). Current hotspots of lncRNA research focus mainly on tumorigenesis and stem cell pluripotency, while little is known about the role of lncRNAs in myogenesis, especially regarding their regulation of muscle mass. Using microarrays, Zhu et al. (29) identified 82 lncRNAs that are differentially expressed in original and differentiated muscle stem cells and revealed that the lncRNA *lnc-mg* regulates muscle mass at the individual animal level. In this study, we used microarray analysis to systematically analyze the expression profiles of lncRNAs during C2C12 cell differentiation and identified 356 persistently up-regulated and 266 persistently down-regulated lncRNAs. Our results provided a database to further screen functional lncRNAs that are involved in muscle fiber formation. Based on this database, we identified the

lncRNA *SYISL* as a repressor of muscle development and found that *SYISL* KO significantly increased the number of smaller muscle fibers and muscle mass in mice. In general, muscle mass is determined by the number and size of muscle fibers. An increase in the size or cross-sectional area of muscle cells is deemed muscle hypertrophy, whereas hyperplasia involves an increase in the number of muscle cells (3, 46). Thus, we concluded that the increased muscle mass observed in *SYISL*-KO mice results mainly from muscle hyperplasia rather than from hypertrophy.

PRC2 is involved in various biological processes, including cell proliferation, differentiation, stem cell maintenance, and embryonic development, and myogenic differentiation is controlled by PRC2-mediated pathways (47–49). In undifferentiated myoblasts, PRC2 and HDAC1 are detected in the genomic regions of silent muscle-specific genes. By contrast, PRC2 dissociates from muscle-specific gene loci, and then MyoD and SRF are recruited to chromatin in differentiated myotubes (10). PRC-mediated gene silencing is mainly dependent on the regulation of EZH2-mediated H3K27me3 (50–52). In addition, the lncRNAs *Xist*, *HOTAIR*, *H19*, *Chaer*, *Fendrr*, *Braveheart*, and *linc-YY1* are involved in the recruitment of PRC2 to the specific regulatory regions (25, 38, 53, 54). For example, the long intergenic noncoding RNA *HOTAIR* recruits PRC2 to specific target genes, leading to the trimethylation of H3K27 and epigenetic silencing of metastasis-suppressor genes (55). *Linc-YY1* interacts with YY1/PRC2, evicts YY1/PRC2 from target promoters, and activates the expression of target genes (25). Here, we located EZH2-binding peaks within the promoters of 36 genes regulated by *SYISL*. Functional analysis further confirmed that *SYISL* recruits PRC2 to the promoters of its target genes and inhibits their expression through EZH2-mediated H3K27me3. Meanwhile, our results indicated that *SYISL* is indispensable for the repression of myogenic gene expression mediated by PRC2. Previous studies showed that mice with conditional knockout (cKO) of *EZH2* in satellite cells have reduced muscle mass with smaller myofibers and compromised muscle regeneration (12), the opposite of the muscle phenotype of *SYISL*-KO mice. *EZH2* cKO in mice results in impaired satellite-cell proliferation characterized by a reduction of $Pax7^+$ cells and derepression of genes expressed in nonmuscle cell lineages (12), which may account for the reduction of muscle mass and regeneration. Interestingly, *SYISL*-KO mice show significantly increased muscle fiber density and muscle mass although myoblast proliferation is partly arrested. We speculate that the increased muscle density and mass of *SYISL*-KO mice are mainly caused by the elimination of *SYISL*'s inhibition of the expression of myogenic genes such as *MyoG*. Indeed, because the *SYISL* expression level increases significantly with myogenic differentiation in normal conditions, *SYISL* may play more important roles in the inhibition of myogenic differentiation than in the promotion of myoblast proliferation by recruiting EZH2 to target gene promoters or other mechanisms. Moreover, full-length *SYISL* is required for its physical interaction with EZH2 to repress the expression of target genes. Recent studies have reported that secondary and tertiary lncRNA structures might be correlated with their biological functions and protein-binding potential (56). Thus, we assume that full-length *SYISL* may be necessary for the formation of secondary or higher-order structures to interact with its binding proteins. Our results supply evidence that lncRNAs are involved in the PRC2-mediated epigenetic regulation of myoblast proliferation and differentiation.

Myoblast fusion is also a critical process that contributes to muscle growth and regeneration and that is controlled by multiple molecular and signaling pathways, such as the Myomaker, Kif2, Cav2, Trio, Cdh18, Itgb1, MAPK, Wnt, and calcineurin-NFATc2 pathways (57). In this study, the microarray data and qPCR results showed that *SYISL* knockdown reduces the expression of some myocyte fusion-associated genes, including *Myomaker*, *β-1 integrin*, *Kif2*, *Cav2*, *Trio*, *Cdh18*, and *Itgb1*. However, no EZH2-binding peaks exist within the promoters of these genes, according to the EZH2 and H3K27me3 ChIP-seq data. Additionally, only a subset of genes is coregulated by the *SYISL* and *EZH2* genes. Thus, we hypothesize that during myogenesis *SYISL* may regulate the expression of some target genes, particularly genes related to myoblast fusion, through other mechanisms. lncRNAs were found to interact with multiple proteins (58). For example, *Xist* interacts with 81 proteins from the chromatin-modification, nuclear-matrix, and RNA-remodeling pathways (59). Similarly, like PRC2, other unknown proteins may participate in *SYISL*-mediated myogenesis. Beyond that, lncRNAs have been shown to function as miRNA molecular sponges to affect the expression of miRNA target genes (34). For instance, *MALAT1* has been identified as a *miR-133* molecular sponge (60), and *lnc-mg* functions as a competing endogenous RNA for *miR-125b* (29). Bioinformatics analysis showed the *SYISL* sequence also contains multiple potential miRNA-binding sites, such as sites for *miR-1*, *miR-125*, *miR-214*, *miR-133*, and *miR-124*, which are involved in the regulation of myogenic differentiation (61). Therefore, *SYISL* could feasibly exert its function by acting as miRNA sponge.

Compared with protein-coding genes, lncRNAs show lower conservation across species, especially in their nucleotide sequences. However, recent studies have indicated that lncRNAs exhibit cross-species conservation of their genomic position (62). For example, *LncMyoD* is located ∼30 kb upstream of the mouse *MyoD* gene, and in the human genome a conserved lncRNA (termed "*hLncMyoD*") was identified ∼20 kb upstream of the human *MyoD* gene (26). Likewise, both human and mouse *linc-YY1* are transcribed from the upstream genomic regions of *YY1* (25). Bioinformatics analysis indicated that the human lncRNA *AK021986* is transcribed from the fourth intron of the *SYNPO2* gene (*SI Appendix*, Fig. S15*A*). We next analyzed the expression pattern of *AK021986* in human normal tissues using the AnnoLnc web server and found that *AK021986* is highly expressed in skeletal muscle (*SI Appendix*, Fig. S15*B*), a pattern similar to that of mouse *SYISL*. In addition, human *AK021986* is mainly expressed in the nuclei of human ES cells and SK.N.SH cells, as determined using the lncATLAS annotation database (*SI Appendix*, Fig. S15 *C* and *D*). Recent studies have revealed that PRC2-binding lncRNAs have distinctive and evolutionarily conserved sequence features across species (63). Thus, we analyzed the binding capacity of *AK021986* and PRC2 using the lncPro calculation method (64). Interestingly, human *AK021986* shows a higher interaction score with PRC2 than the known PRC2-binding lncRNA *HOTAIR* (*SI Appendix*, Fig. S15*E*). Considering the important roles of *SYISL* in muscle development, further elucidation of the function and mechanism of *AK021986* in human muscle development will be worthwhile.

In summary, we identify an lncRNA, *SYISL*, and propose a mechanistic model to elucidate its role in the regulation of muscle fiber formation through PRC2-mediated epigenetic silencing (*SI Appendix*, Fig. S16). At the individual animal level, *SYISL* cKO in mice leads to increased muscle fiber density and muscle mass. Mechanistically, on the one hand, *SYISL* recruits PRC2 to repress *p21* gene expression, resulting in failure to exit the cell cycle and promotion of myoblast proliferation. On the other hand, *SYISL* guides PRC2 to repress the expression of muscle-specific genes, such as *MyoG* and *Myh4*, and restrains myoblast differentiation. Meanwhile, *SYISL* increases the rate of myocyte fusion by other unknown mechanisms.

Materials and Methods

The lncRNA *SYISL* was screened using microarray analysis, and its function was identified by gene overexpression and interference experiments in myoblasts. *SYISL*-KO mice were generated using the CRISPR/Cas9 system. Muscle fiber and regeneration phenotypes were measured to verify the

effects of *SYISL* on myogenesis. Animal experiments were conducted based on the National Research Council Guide for the Care and Use of Laboratory Animals and approved by the Institutional Animal Care and Use Committee at Huazhong Agricultural University. The molecular mechanism by which *SYISL* regulates target gene expression was examined by RIP, RNA pulldown, ChIRP, ChIP, and other methods. See *SI Appendix* for detailed information.

ACKNOWLEDGMENTS. We thank Dr. Wang Fengchao for helping in the generation of *SYISL*-KO mice and Dr. Wang Heng for helping in muscle regeneration experiments. This work was supported by National Project for Breeding of Transgenic Pig Grants 2016ZX08006-002 and 2018ZX080102B-002, Fundamental Research Funds for Central Universities Grant 2662018PY045, the National Natural Science Foundation of China Grant 91440114, and the Agricultural Innovation Fund of Hubei Province (B.Z.).

1. Buckingham M (2006) Myogenic progenitor cells and skeletal myogenesis in vertebrates. *Curr Opin Genet Dev* 16:525–532.
2. Buckingham M, Rigby PW (2014) Gene regulatory networks and transcriptional mechanisms that control myogenesis. *Dev Cell* 28:225–238.
3. Braun T, Gautel M (2011) Transcriptional mechanisms regulating skeletal muscle differentiation, growth and homeostasis. *Nat Rev Mol Cell Biol* 12:349–361.
4. Liu QC, et al. (2012) Comparative expression profiling identifies differential roles for myogenin and p38α MAPK signaling in myogenesis. *J Mol Cell Biol* 4:386–397.
5. Albini S, et al. (2013) Epigenetic reprogramming of human embryonic stem cells into skeletal muscle cells and generation of contractile myospheres. *Cell Rep* 3:661–670.
6. Perdiguero E, Sousa-Victor P, Ballestar E, Muñoz-Cánoves P (2009) Epigenetic regulation of myogenesis. *Epigenetics* 4:541–550.
7. Bharathy N, Ling BM, Taneja R (2013) Epigenetic regulation of skeletal muscle development and differentiation. *Subcell Biochem* 61:139–150.
8. Asp P, et al. (2011) Genome-wide remodeling of the epigenetic landscape during myogenic differentiation. *Proc Natl Acad Sci USA* 108:E149–E158.
9. Blais A, van Oevelen CJ, Margueron R, Acosta-Alvear D, Dynlacht BD (2007) Retinoblastoma tumor suppressor protein-dependent methylation of histone H3 lysine 27 is associated with irreversible cell cycle exit. *J Cell Biol* 179:1399–1412.
10. Caretti G, Di Padova M, Micales B, Lyons GE, Sartorelli V (2004) The polycomb Ezh2 methyltransferase regulates muscle gene expression and skeletal muscle differentiation. *Genes Dev* 18:2627–2638.
11. Stojic L, et al. (2011) Chromatin regulated interchange between polycomb repressive complex 2 (PRC2)-Ezh2 and PRC2-Ezh1 complexes controls myogenin activation in skeletal muscle cells. *Epigenetics Chromatin* 4:16.
12. Juan AH, et al. (2011) Polycomb EZH2 controls self-renewal and safeguards the transcriptional identity of skeletal muscle stem cells. *Genes Dev* 25:789–794.
13. Woodhouse S, Pugazhendhi D, Brien P, Pell JM (2013) Ezh2 maintains a key phase of muscle satellite cell expansion but does not regulate terminal differentiation. *J Cell Sci* 126:565–579.
14. Brockdorff N, et al. (1991) Conservation of position and exclusive expression of mouse Xist from the inactive X chromosome. *Nature* 351:329–331.
15. Zhang H, et al. (2014) Long noncoding RNA-mediated intrachromosomal interactions promote imprinting at the Kcnq1 locus. *J Cell Biol* 204:61–75.
16. Gabory A, et al. (2009) H19 acts as a trans regulator of the imprinted gene network controlling growth in mice. *Development* 136:3413–3421.
17. Tripathi V, et al. (2010) The nuclear-retained noncoding RNA MALAT1 regulates alternative splicing by modulating SR splicing factor phosphorylation. *Mol Cell* 39: 925–938.
18. Hu S, Shan G (2016) LncRNAs in stem cells. *Stem Cells Int* 2016:2681925.
19. Chen L, Zhang S (2016) Long noncoding RNAs in cell differentiation and pluripotency. *Cell Tissue Res* 366:509–521.
20. Bhan A, Mandal SS (2014) Long noncoding RNAs: Emerging stars in gene regulation, epigenetics and human disease. *ChemMedChem* 9:1932–1956.
21. Wapinski O, Chang HY (2011) Long noncoding RNAs and human disease. *Trends Cell Biol* 21:354–361.
22. Schmitt AM, Chang HY (2016) Long noncoding RNAs in cancer pathways. *Cancer Cell* 29:452–463.
23. Neguembor MV, Jothi M, Gabellini D (2014) Long noncoding RNAs, emerging players in muscle differentiation and disease. *Skelet Muscle* 4:8.
24. Wang L, et al. (2015) LncRNA Dum interacts with Dnmts to regulate Dppa2 expression during myogenic differentiation and muscle regeneration. *Cell Res* 25:335–350.
25. Zhou L, et al. (2015) Linc-YY1 promotes myogenic differentiation and muscle regeneration through an interaction with the transcription factor YY1. *Nat Commun* 6: 10026.
26. Gong C, et al. (2015) A long non-coding RNA, LncMyoD, regulates skeletal muscle differentiation by blocking IMP2-mediated mRNA translation. *Dev Cell* 34:181–191.
27. Mueller AC, et al. (2015) MUNC, a long noncoding RNA that facilitates the function of MyoD in skeletal myogenesis. *Mol Cell Biol* 35:498–513.
28. Yu X, et al. (2017) Long non-coding RNA Linc-RAM enhances myogenic differentiation by interacting with MyoD. *Nat Commun* 8:14016.
29. Zhu M, et al. (2017) Lnc-mg is a long non-coding RNA that promotes myogenesis. *Nat Commun* 8:14718.
30. Martinet C, et al. (2016) H19 controls reactivation of the imprinted gene network during muscle regeneration. *Development* 143:962–971.
31. Chen X, et al. (2017) *Malat1* regulates myogenic differentiation and muscle regeneration through modulating MyoD transcriptional activity. *Cell Discov* 3:17002.
32. Weirick T, John D, Dimmeler S, Uchida S (2015) C-It-Loci: A knowledge database for tissue-enriched loci. *Bioinformatics* 31:3537–3543.
33. Zeng W, et al. (2016) Single-nucleus RNA-seq of differentiating human myoblasts reveals the extent of fate heterogeneity. *Nucleic Acids Res* 44:e158.
34. Chen LL (2016) Linking long noncoding RNA localization and function. *Trends Biochem Sci* 41:761–772.
35. Engreitz JM, et al. (2016) Local regulation of gene expression by lncRNA promoters, transcription and splicing. *Nature* 539:452–455.
36. Qin CY, Cai H, Qing HR, Li L, Zhang HP (2017) Recent advances on the role of long non-coding RNA H19 in regulating mammalian muscle growth and development. *Yi Chuan* 39:1150–1157.
37. Pereira JD, et al. (2010) Ezh2, the histone methyltransferase of PRC2, regulates the balance between self-renewal and differentiation in the cerebral cortex. *Proc Natl Acad Sci USA* 107:15957–15962.
38. Davidovich C, Cech TR (2015) The recruitment of chromatin modifiers by long noncoding RNAs: Lessons from PRC2. *RNA* 21:2007–2022.
39. Xu T, Jiang W, Fan L, Gao Q, Li G (2017) Upregulation of long noncoding RNA Xist promotes proliferation of osteosarcoma by epigenetic silencing of P21. *Oncotarget* 8: 101406–101417.
40. Zhang F, Peng H (2017) LncRNA-ANCR regulates the cell growth of osteosarcoma by interacting with EZH2 and affecting the expression of p21 and p27. *J Orthop Surg Res* 12:103.
41. Negishi M, et al. (2014) A new lncRNA, APTR, associates with and represses the CDKN1A/p21 promoter by recruiting polycomb proteins. *PLoS One* 9:e95216.
42. Latres E, et al. (2000) Limited overlapping roles of P15(INK4b) and P18(INK4c) cell cycle inhibitors in proliferation and tumorigenesis. *EMBO J* 19:3496–3506.
43. Grange M, et al. (2015) Control of CD8 T cell proliferation and terminal differentiation by active STAT5 and CDKN2A/CDKN2B. *Immunology* 145:543–557.
44. Fatica A, Bozzoni I (2014) Long non-coding RNAs: New players in cell differentiation and development. *Nat Rev Genet* 15:7–21.
45. Li J, Tian H, Yang J, Gong Z (2016) Long noncoding RNAs regulate cell growth, proliferation, and apoptosis. *DNA Cell Biol* 35:459–470.
46. Otto A, Patel K (2010) Signalling and the control of skeletal muscle size. *Exp Cell Res* 316:3059–3066.
47. Aloia L, Di Stefano B, Di Croce L (2013) Polycomb complexes in stem cells and embryonic development. *Development* 140:2525–2534.
48. Boyer LA, et al. (2006) Polycomb complexes repress developmental regulators in murine embryonic stem cells. *Nature* 441:349–353.
49. Khan AA, Lee AJ, Roh TY (2015) Polycomb group protein-mediated histone modifications during cell differentiation. *Epigenomics* 7:75–84.
50. Margueron R, Reinberg D (2011) The polycomb complex PRC2 and its mark in life. *Nature* 469:343–349.
51. Schuettengruber B, Cavalli G (2009) Recruitment of polycomb group complexes and their role in the dynamic regulation of cell fate choice. *Development* 136:3531–3542.
52. Simon JA, Kingston RE (2009) Mechanisms of polycomb gene silencing: Knowns and unknowns. *Nat Rev Mol Cell Biol* 10:697–708.
53. Wang Z, et al. (2016) The long noncoding RNA Chaer defines an epigenetic checkpoint in cardiac hypertrophy. *Nat Med* 22:1131–1139.
54. Grote P, et al. (2013) The tissue-specific lncRNA Fendrr is an essential regulator of heart and body wall development in the mouse. *Dev Cell* 24:206–214.
55. Gupta RA, et al. (2010) Long non-coding RNA HOTAIR reprograms chromatin state to promote cancer metastasis. *Nature* 464:1071–1076.
56. Li R, Zhu H, Luo Y (2016) Understanding the functions of long non-coding RNAs through their higher-order structures. *Int J Mol Sci* 17:E702.
57. Hindi SM, Tajrishi MM, Kumar A (2013) Signaling mechanisms in mammalian myoblast fusion. *Sci Signal* 6:re2.
58. Khalil AM, et al. (2009) Many human large intergenic noncoding RNAs associate with chromatin-modifying complexes and affect gene expression. *Proc Natl Acad Sci USA* 106:11667–11672.
59. Chu C, et al. (2015) Systematic discovery of Xist RNA binding proteins. *Cell* 161: 404–416.
60. Han X, Yang F, Cao H, Liang Z (2015) Malat1 regulates serum response factor through miR-133 as a competing endogenous RNA in myogenesis. *FASEB J* 29:3054–3064.
61. Luo W, Nie Q, Zhang X (2013) MicroRNAs involved in skeletal muscle differentiation. *J Genet Genomics* 40:107–116.
62. Ulitsky I, Shkumatava A, Jan CH, Sive H, Bartel DP (2011) Conserved function of lincRNAs in vertebrate embryonic development despite rapid sequence evolution. *Cell* 147:1537–1550.
63. Tu S, Yuan GC, Shao Z (2017) The PRC2-binding long non-coding RNAs in human and mouse genomes are associated with predictive sequence features. *Sci Rep* 7:41669.
64. Lu Q, et al. (2013) Computational prediction of associations between long non-coding RNAs and proteins. *BMC Genomics* 14:651.